

Detection Of Short-Circuits Of Dc Motor Using Thermographic Images, Binarization and K-Nn Classifier

HIMANSU SEKHAR MAHARANA ¹ SANJAY KUMAR NAYAK ² SUNITA
BARAL ³ CHINMAYA RANJAN PRADHAN ⁴

Department of Electrical Engineering, Aryan Institute of Engineering & Technology, Bhubaneswar

Department of Electrical Engineering, Raajdhani Engineering College, Bhubaneswar

Department of Electrical Engineering, Capital Engineering College, Bhubaneswar

Department of Electrical Engineering, NM Institute of Engineering & Technology, Bhubaneswar

Many fault diagnostic methods have been developed in recent years. One of them is thermography. It is a safe and non-invasive method of diagnostic. Fault diagnostic method of incipient states of Direct Current motor was described in the article. Thermographic images of the commutator of Direct Current motor were used in an analysis. Two kinds of thermographic images were analysed: thermographic image of commutator of healthy DC motor, thermographic image of commutator of DC motor with shorted rotor coils. The analysis was carried out for image processing methods such as: extraction of magenta colour, binarization, sum of vertical pixels and sum of all pixels in the image. Classification was conducted for K-Nearest Neighbour classifier. The results of analysis show that the proposed method is efficient. It can be also used for diagnostic purposes in industrial plants.

Keywords: *diagnostics; DC motor; K-NN classifier; maintenance; thermographic images*

I. INTRODUCTION

Thermal radiation is produced by any object whose temperature is warmer than absolute zero (-273.15°C). Thermography is the process of acquisition of thermographic images. In order to identify and analyze thermal anomalies, it is beneficial to use thermography. Thermography allows locating temperature differences of parts of electrical motors. The faulty states of operations of electrical motors are associated with the thermal anomalies. For example shorted rotor coils of electrical motor cause temperature increase. Next this heat is liberated at a rate greater than in the surrounding area. Faulty states are usually caused by friction, misalignment, worn components, deteriorated connections, short circuits, overloads and load imbalances. Thermography can help detect costly failure before it appears [1÷7]. It is very common to find a loose connection that can be repaired inexpensively. If the electrical motor is allowed to fail, the cost could be high for replacement. The failure of the motor could also result in a major production outage [1]. Fault diagnostic methods and online monitoring were developed for various purposes in the literature [8÷20]. Fault diagnostic methods of rotating machines based on electrical, acoustic and thermal signals were also described [21÷32]. Of course the best diagnostic systems should use all of them. In this paper, the authors proposed a new method of fault diagnostics of thermographic images of DC motor (Fig. 1).

The article is divided in 4 different sections. Section 1 presents applications of thermography and literature survey of fault diagnostic methods of electrical machines. Section 2 describes the proposed method of fault diagnostics. Section 3 presents analysis of thermographic images of DC motor. Section 4 describes conclusions and proposition for future researches.



Figure 1 Analyzed Direct Current motor

II. FAULT DIAGNOSTIC METHOD OF THERMOGRAPHIC IMAGES OF DC MOTOR

Fault diagnostic method of thermographic images of DC motor is presented in Fig. 2. The method started with recording a sequence of thermographic images by using thermographic camera. Next recorded sequence was split into thermographic images. After that extraction of magenta color and binarization were performed. Next feature vectors were formed. These feature vectors (processed samples) belonged to training set and test set. Training set was used to create patterns (Patterns creation). Test set was used by K-Nearest Neighbor classifier (Identification). In the identification step feature vectors from test set were compared with feature vectors from training set. The result of the recognition was the name of the state of DC motor, for example "healthy DC motor" or "DC motor with shorted rotor coils".

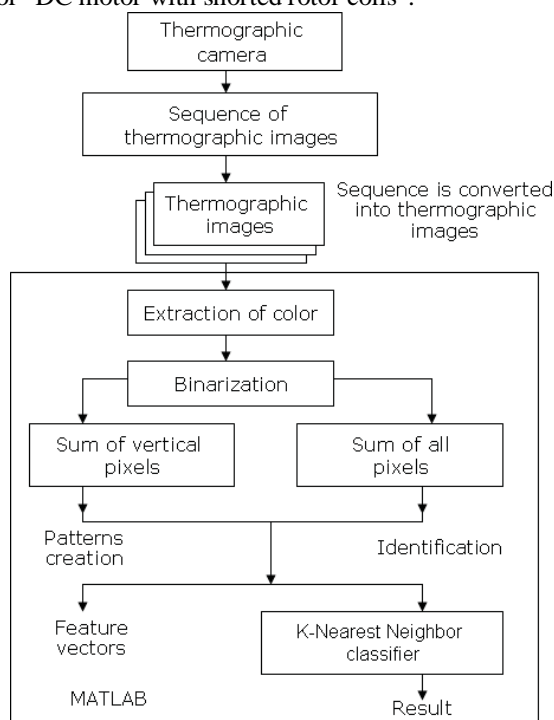


Figure 2 Fault diagnostic method of thermographic images of DC motor using extraction of color, binarization, sum of vertical pixels, sum of all pixels, K-Nearest Neighbor classifier

2.1 Recording of a sequence of thermographic images

Thermographic camera was used for recording of a sequence of thermographic images. It was installed 0.3 m in front of commutator of DC motor (Fig. 3).



Figure 3 Commutator of healthy DC motor

Obtained thermographic images had a resolution of 720×576 pixels (Fig. 4a, 5a). Sequence of images was saved with a resolution of 24 bits (16 777 216 of colors). This sequence of thermographic images was saved on a PC in AVI (Audio Video Interleave) format. The frame rate was equal to 9 Hz.

2.2 Acquisition of thermographic images

1 second of sequence of thermographic images had 9 images (9 Hz). This sequence had 5 seconds, so 45 thermographic images were obtained for each state of DC motor. To obtain thermographic image *mplayer* library was used. *Mplayer* could split sequence of thermographic images into a certain number of images, depending on the parameters of the sequence.

2.3 Extraction of magenta colour

MATLAB software was used to extract magenta color from the image. MATLAB used CMY color model, so the image consisted of 3 colors: cyan, magenta and yellow (CMY). On the obtained images higher temperatures were marked by red. Red consisted of magenta and yellow. Lower temperatures were marked by blue. Average temperatures were marked by yellow. It was noticed that magenta had the biggest influence on higher temperatures, so only this color was analyzed. There are more solutions of this problem for example using RGB color space.

Thermographic images and magenta color of images of commutator of DC motor are presented in Figs. 4÷5. Figs. 4b and 5b are monochrome images.

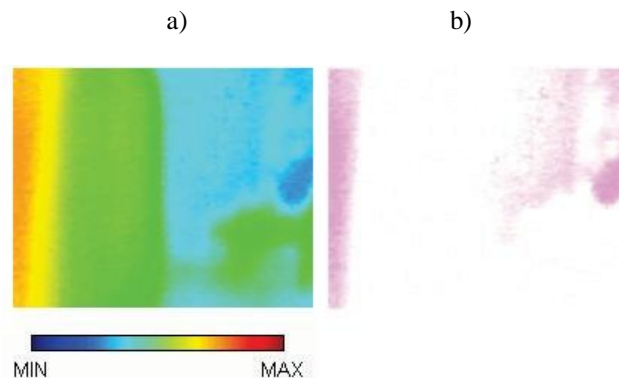


Figure 4 a) Thermographic image of commutator of healthy DC motor,
b) Magenta color of thermographic image of commutator of healthy DC motor

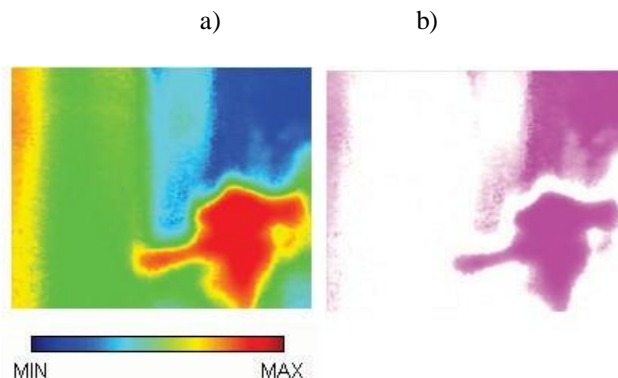


Figure 5 a) Thermographic image of commutator of shorted DC motor,
 b) Magenta color of thermographic image of commutator of shorted DC motor

2.4 Binarization

Image binarization converted grayscale image into binary image using a thresholding operation. The method replaced each pixel in an image with a black pixel or white pixel depending on threshold value [28]. In this paper, the authors used threshold below, $I < T$, where I - image intensity, T - threshold. If I was less than T then I was replaced by white pixel (value 1). To choose the correct binarization threshold T , analysis was performed using sum of vertical pixels, sum of all pixels and K-NN classifier ($K=1$). $EoRoCTI$ was defined by formula (2) in Section 3. In analysis, the authors set $T = 0.1$ in the range $<0,1>$, however another binarization threshold T (Tab. 1) will also give good results.

Table 1 Results of recognition of thermographic images of DC motor using sum of vertical pixels, sum of all pixels and K-NN classifier depending on binarization threshold T

$K=1$	$T=0.001$	$T=0.01$	$T=0.1$
$EoRoCTI$ (%)	100	100	100
$K=1$	$T=0.3$	$T=0.5$	$T=0.7$
$EoRoCTI$ (%)	100	100	100
$K=1$	$T=0.9$	$T=0.99$	$T=0.999$
$EoRoCTI$ (%)	100	100	100

Magenta color of thermographic images of commutator of DC motor after binarization for $T = 0.1$ is presented in Fig. 6.

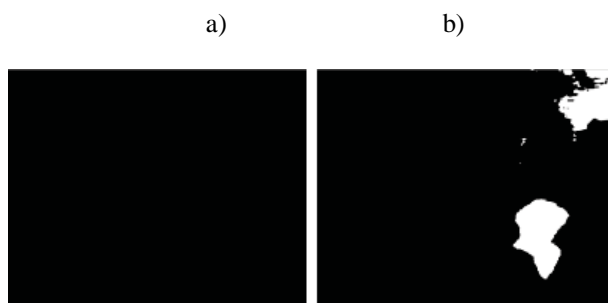


Figure 6 a) Magenta color of thermographic image of commutator of healthy DC motor after binarization for $T = 0.1$, b) Magenta color of thermographic image of commutator of shorted DC motor after binarization for $T = 0.1$

2.5 Feature vectors

Feature extraction of images was described in the literature [33÷37]. In this paper, the authors proposed the

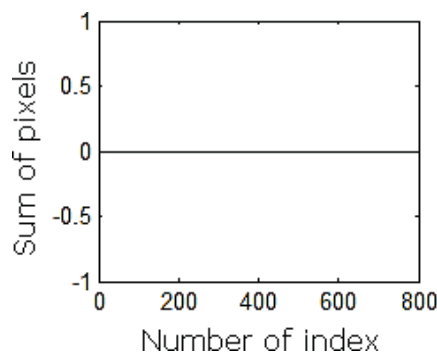


Figure 7 Feature vector of binary image of healthy DC motor

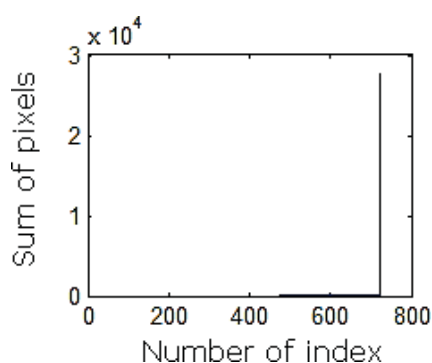


Figure 8 Feature vector of binary image of DC motor with shorted rotor coils

2.6 K-Nearest Neighbor classifier

Classification of data was discussed in the literature. Many methods of classification were developed such as: K-Nearest Neighbor, Nearest Mean, Backpropagation Neural Network, classifier based on words, Fuzzy Logic, Genetic algorithms, Support Vector Machine, decision tree [38÷56]. The K-NN classifier was very good to classify high dimensional feature vector - 721 dimensions. The mentioned classifier could be used with various distance functions such as: Manhattan, Euclidean, Minkowski, Jacquard distance. The results of these functions were very similar, so in conducted analysis Manhattan distance was used. Manhattan distance d_m was defined as the distance between two feature vectors. For feature vectors $sva = [sva_1, sva_2, \dots, sva_n]$ and $svb = [svb_1, svb_2, \dots, svb_n]$ it was expressed by formula (1):

$$d_m(sva, svb) = \sum_{i=1}^n |sva_i - svb_i| \quad (1)$$

When all distances for test and training samples were calculated. The majority decision rule was used to identify the state of DC motor.

III. ANALYSIS OF RECOGNITION OF THERMOGRAPHIC IMAGES OF COMMUTATOR OF DC MOTOR

Analysis of recognition of thermographic images of commutator of DC motor was conducted for 2 states of motor: healthy DC motor, shorted DC motor (Fig. 9a, 9b). Analyzed DC motor was powered by a generator. Analyzed DC motor had following operation parameters:

$$P_{Nom} = 13 \text{ kW}, U_{Nom} = 75 \text{ V}, U_{AG} = 170 \text{ V}, I_{shorted} = 420$$

$$\text{A}, R_{shorted} = 4 \text{ m}\Omega, V_s = 700 \text{ rpm.}$$

Where P_{Nom} - motor power, U_{Nom} - nominal motor voltage, U_{AG} - voltage of the generator, $I_{shorted}$ - short-circuit current, $R_{shorted}$ - short-circuit resistance, V_s - rotor speed.

Group of three loops of rotor coils were shorted. It is presented in Fig. 9b.

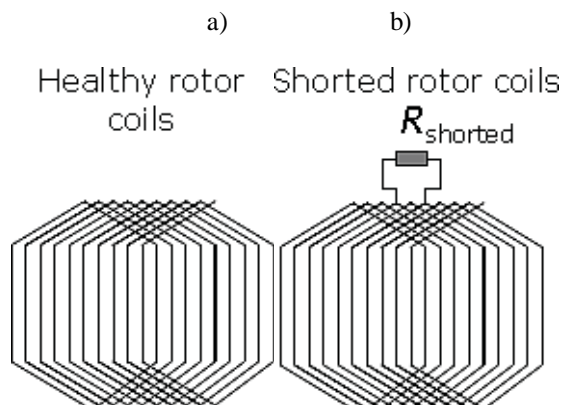


Figure 9 a) Scheme of rotor windings of healthy DC motor, b) Scheme of rotor windings of DC motor with 3 shorted rotor coils

Analysis was conducted for 80 test samples and 10 training samples (thermographic images). Efficiency of recognition of thermographic image was expressed by:

$$EoRoCTI = \frac{NoTCTI}{NoATCTI} 100\% \quad (2)$$

Where: *EoRoCTI* – efficiency of recognition of thermographic image, *NoTCTI* – number of test thermographic images (test samples) identified properly, *NoATCTI* – number of all test thermographic images.

The results of recognition of thermographic images of commutator of DC motor are presented in Tabs. 2 and 3. Value of *EoRoCTI* was in range of 92.5÷100 % for feature vector consisted of sum of vertical pixels and sum of all pixels (Tab. 2). Value of *EoRoCTI* was in range of 90÷100 % for feature vector only consisted of sum of vertical pixels (Tab. 3).

Table 2 Results of recognition of thermographic images of commutator of DC motor using sum of vertical pixels, sum of all pixels and K-NN classifier depending on parameter *K*

	State of DC motor	<i>EoRoCTI</i> (%)
<i>K</i> =1	Healthy DC motor	100
	Shorted DC motor	100
<i>K</i> =3	Healthy DC motor	100
	Shorted DC motor	100
<i>K</i> =5	Healthy DC motor	100
	Shorted DC motor	92.5

Table 3 Results of recognition of thermographic images of commutator of DC motor using sum of vertical pixels and K-NN classifier depending on parameter *K*

	State of DC motor	<i>EoRoCTI</i> (%)
<i>K</i> =1	Healthy DC motor	100
	Shorted DC motor	100
<i>K</i> =3	Healthy DC motor	100
	Shorted DC motor	100
<i>K</i> =5	Healthy DC motor	100
	Shorted DC motor	90

IV. CONCLUSIONS

In this paper, the authors presented diagnostic system. The authors conducted analysis of thermographic images of commutator of DC motor. A new method of feature extraction of thermographic images was proposed. This method was based on sum of vertical pixels and sum of all pixels. Next feature vectors were classified by K-NN classifier. Obtained results of analysis were very good for two states of DC motor.

Detecting differences of temperature is the main advantage of thermography. Moreover it is also non-invasive method of fault diagnostics. Unfortunately thermographic camera is very expensive. It costs about 1000÷5000 \$. The second disadvantage of the method based on thermography is that DC motor takes time to warm up. However thermographic images can be used for monitoring of DC motors with the same type, size,

operation parameters. Thermography can be also used together with other signals such as: electric and acoustic. Future researches may lead to developing a reliable diagnostic method of rotating electrical motors.

ACKNOWLEDGEMENTS

This work has been financed under AGH University of Science and Technology, AGH researcher grant in 2017 (Adam Glowacz).

REFERENCES

- [1]. Allianz Global Corporate & Specialty. Infrared
- [2]. Thermography: Determining failure or problems in electrical systems. // Risk Bulletin. No. 38 (2011).
- [3]. Singh, G.; Kumar, T. C. A.; Naikan, V. N. A. Induction motor inter turn fault detection using infrared thermographic analysis. // Infrared Physics & Technology. 77, (2016), pp. 277-282. <https://doi.org/10.1016/j.infrared.2016.06.010>
- [4]. Liu, T.; Zhang, W.; Yan, S. Z. A novel image enhancement algorithm based on stationary wavelet transform for infrared thermography to the de-bonding defect in solidrocket motors. // Mechanical Systems and Signal Processing. 62-63, (2015), pp. 366-380. <https://doi.org/10.1016/j.ymssp.2015.03.010>
- [5]. Glowacz, A.; Glowacz, A.; Glowacz, Z. Diagnostics of Direct Current generator based on analysis of monochrome infrared images with the application of cross-sectional image and nearest neighbor classifier with Euclidean distance. // Przegląd Elektrotechniczny. 88, 6(2012), pp.154-157.
- [6]. Koprowski, R. Some selected quantitative methods of thermal image analysis in Matlab. // Journal of Biophotonics. 9, 5(2016), pp. 510-520. <https://doi.org/10.1002/jbio.201500224>
- [7]. Jaffery, Z. A.; Dubey, A. K.; Irshad; Haque, A. Scheme for predictive fault diagnosis in photo-voltaic modules using thermal imaging. // Infrared Physics & Technology. 83, (2017), pp. 182-187. <https://doi.org/10.1016/j.infrared.2017.04.015>
- [8]. Sebok, M.; Gutton, M.; Kucera, M. Diagnostics of electric equipments by means of thermovision. // Przegląd Elektrotechniczny. 87, 10(2011), pp. 313-317.
- [9]. Hreha, P.; Radvanska, A.; Knapcikova, L.; Krolczyk, G. M.; Legutko, S.; Krolczyk, J. B.; Hloch, S.; Monka, P. Roughness Parameters Calculation By Means Of On-Line Vibration Monitoring Emerging From AWJ Interaction With Material. // Metrology and Measurement Systems. 22,2(2015), pp. 315-326. <https://doi.org/10.1515/mms-2015-0024>
- [10]. Li, Z. X.; Sheng, C. X.; Li, Y. J.; Xing, J. T.; Su, B. Y. Efficient Fault Feature Extraction and Fault Isolation for High Voltage DC Transmissions. // Elektronika Ir Elektrotechnika. 21, 5(2015), pp. 7-12. <https://doi.org/10.5755/j01.eee.21.5.13317>
- [11]. Li, Z. X.; Yan, X. P.; Wang, X. P.; Peng, Z. X. Detection of gear cracks in a complex gearbox of wind turbines using supervised bounded component analysis of vibration signals collected from multi-channel sensors. // Journal of Sound and Vibration. 371, (2016), pp. 406-433. <https://doi.org/10.1016/j.jsv.2016.02.021>
- [12]. Sun, Y.; Zhang, Y. G.; Wang, Y. D. Research on the Fault Coefficient in Complex Electrical Engineering. // Applied Sciences-Basel. 5, 3(2015), pp. 307-319. <https://doi.org/10.3390/app5030307>
- [13]. Sawczuk, W.; Szymanski, G. M. Diagnostics of the railway friction disc brake based on the analysis of the vibration signals in terms of resonant frequency. // Archive of Applied Mechanics. 87, 5(2017), pp. 801-815. <https://doi.org/10.1007/s00419-016-1202-0>
- [14]. Sawczuk, W. The Application of Vibration Accelerations in the Assessment of Average Friction Coefficient of a Railway Brake Disc. // Measurement Science Review. 17, 3(2017), pp. 125-134. <https://doi.org/10.1515/msr-2017-0016>
- [15]. Michalak, M.; Sikora, M.; Sobczyk, J. Analysis of the longwall conveyor chain based on a harmonic analysis. // Eksploatacja i Niezawodność – Maintenance and Reliability. 15, 4(2013), pp. 332-336.
- [16]. Li, Z. X.; Jiang, Y.; Hu, C.; Peng, Z. Recent progress on decoupling diagnosis of hybrid failures in gear transmission systems using vibration sensor signal: A review. // Measurement. 90, (2016), pp. 4-19. <https://doi.org/10.1016/j.measurement.2016.04.036>
- [17]. Deptula, A.; Kunderman, D.; Osinski, P.; Radziwanowska, U.; Wlostowski, R. Acoustic Diagnostics Applications in the Study of Technical Condition of Combustion Engine. // Archives of Acoustics. 41, 2(2016), pp. 345-350. <https://doi.org/10.1515/aoa-2016-0036>
- [18]. Deptula, A.; Osinski, P.; Radziwanowska, U. Decision Support System for Identifying Technical Condition of Combustion Engine. // Archives of Acoustics. 41, 3(2016), pp. 449-460.
- [19]. Jedlinski, L.; Caban, J.; Krzywonos, L.; Wierzbicki, S.; Brumerick, F. Application of vibration signal in the diagnosis of IC engine valve clearance. // Journal of Vibroengineering. 17, 1(2015), pp. 175-187.
- [20]. Gutton, M.; Korenciak, D.; Kucera, M.; Sebok, M.; Opielak, M.; Zukowski, P.; Koltunowicz, T. N. Maintenance diagnostics of transformers considering the influence of short-circuit currents during operation. // Eksploatacja i Niezawodność – Maintenance and Reliability. 19, 3(2017), pp. 459-466. <https://doi.org/10.17531/ein.2017.3.17>
- [21]. Jozwik, J. Identification and monitoring of noise sources of CNC machine tools by acoustic holography methods. // Advances in Science and Technology-Research Journal. 10,30(2016), pp. 127-137. <https://doi.org/10.12913/22998624/63386>
- [22]. Lopez-Perez, D.; Antonino-Daviu, J. Application of Infrared Thermography to Failure Detection in Industrial Induction Motors: Case Stories. // IEEE Transactions on Industry Applications. 53, 3(2017), pp. 1901-1908. <https://doi.org/10.1109/TIA.2017.2655008>
- [23]. Garcia-Ramirez, A. G.; Morales-Hernandez, L. A.; Osornio-Rios, R. A.; Benitez-Rangel, J. P.; Garcia-Perez, A.; Romero-Troncoso, R. D. Fault detection in induction motors and the impact on the kinematic chain through thermographic analysis. // Electric Power Systems Research. 114, (2014), pp. 1-9. <https://doi.org/10.1016/j.epr.2014.03.031>
- [24]. Glowacz, A. Diagnostics of Rotor Damages of Three-Phase Induction Motors Using Acoustic Signals and SMOFS-20-EXPANDED. // Archives of Acoustics. 41, 3(2016), pp. 507-515.
- [25]. Glowacz, Z.; Glowacz, A., Simulation language for analysis of discrete-continuous electrical systems (SESL2). // Proceedings of the 26th IASTED International Conference on Modelling, Identification, and Control. Innsbruck, Austria, (2007), pp. 94-99.
- [26]. Duan, L. X.; Yao, M. C.; Wang, J. J.; Bai, T. B.; Zhang, L. B. Segmented infrared image analysis for rotating machinery fault diagnosis. // Infrared Physics & Technology. 77, (2016), pp. 267-276. <https://doi.org/10.1016/j.infrared.2016.06.011>
- [27]. Sulowicz, M.; Weinreb, K.; Mielnik, R.; Zywczyk, T.; Jaraczewski, M. The method of current measurement in the rotor cage bars of prototype induction motor with the use of Rogowski coils. // 2015 International Conference on Information and Digital

- Technologies (IDT). (2015), pp. 357-365.
- [30]. Glowacz, A.; Glowacz, W.; Glowacz, Z. Recognition of armature current of DC generator depending on rotor speed using FFT, MSAF-1 and LDA. // *Eksploracja i Niezawodność – Maintenance and Reliability*. 17, 1(2015), pp. 64-69. <https://doi.org/10.17531/ein.2015.1.9>
- [31]. Glowacz, A.; Glowacz, A.; Glowacz, Z. Recognition of Monochrome Thermal Images of Synchronous Motor with the Application of Skeletonization and Classifier Based on Words. // *Archives of Metallurgy and Materials*. 60, 1(2015), pp. 27-32. <https://doi.org/10.1515/amm-2015-0004>
- [32]. Lim, G. M.; Bae, D. M.; Kim, J. H. Fault diagnosis of rotating machine by thermography method on support vector machine. // *Journal of Mechanical Science and Technology*. 28, 8(2014), pp. 2947-2952. <https://doi.org/10.1007/s12206-014-0701-6>
- [33]. Glowacz, Z. Automatic Recognition of Armature Current of Dc Motor with Application of FFT and GSDM. // *Archives of Metallurgy and Materials*. 56, 1(2011), pp. 25-30. <https://doi.org/10.2478/v10172-011-0003-2>
- [34]. Van Hecke, B.; Yoon, J. Low speed bearing fault diagnosis using acoustic emission sensors. // *Applied Acoustics*. 105,(2016), pp. 35-44. <https://doi.org/10.1016/j.apacoust.2015.10.028>
- [35]. Hemmati, F.; Orfali, W.; Gadala, M. S. Roller bearing acoustic signature extraction by wavelet packet transform, applications in fault detection and size estimation. // *Applied Acoustics*. 104, (2016), pp. 101-118. <https://doi.org/10.1016/j.apacoust.2015.11.003>
- [36]. Jaworek-Korjakowska, J.; Kleczek, P. Automatic Classification of Specific Melanocytic Lesions Using Artificial Intelligence. // *BioMed Research International*. (2016), Article Number: 8934242. <https://doi.org/10.1155/2016/8934242>
- [37]. Stepień, K.; Makiela, W.; Stoic, A.; Samardzic, I. Defining the criteria to select the wavelet type for the assessment of surface quality. // *Tehnicki Vjesnik-Technical Gazette*. 22, 3(2015), pp. 781-784. <https://doi.org/10.17559/TV-20140124110406>
- [38]. Hachaj, T.; Ogiela, M. R. Rule-based approach to recognizing human body poses and gestures in real time. // *Multimedia Systems*. 20, 1(2014), pp. 81-99. <https://doi.org/10.1007/s00530-013-0332-2>
- [39]. Koprowski, R. Automatic analysis of the trunk thermal images from healthy subjects and patients with faulty posture. // *Computers in Biology and Medicine*. 62, (2015), pp. 110-118. <https://doi.org/10.1016/j.compbiomed.2015.04.017>